Supplementary Information (SI) for Journal of Materials Chemistry C.
This journal is © The Royal Society of Chemistry 2025

Supporting information

Hong-Xue Wang[a], Kai-Ni Wei[a]，Qing Tang[b], Zhu Tao[a], Ying Huang[*c]，Qing Chen[*a], Chun Liu[*d]

[a] *Key Laboratory of Macrocyclic and Supramolecular Chemistry of Guizhou Province, Guizhou University, Guiyang 550025, China.*

[b] *Department College of Tobacco Science, Guizhou University, Guiyang 550025, China.*

[c] *The Engineering and Research Center for Southwest Bio-Pharmaceutical Resources of National Education Ministry of China, Guizhou University, Guiyang 550025, China*

[d] *School of culture and tourism, Guiyang Healthcare Vocational University, Guiyang 550081, China*

E-mail: yinghung128@163.com (Y. Huang)

Experimental Section

materials

Q[5], Q[6], Q[7], Q[8], TMeQ[6], HMeQ[6] was prepared and purified according to previously published methods[1, 2]. Fluorescence lifetimes and quantum yields (Φ) were determined using an FLS1000 spectrophotometer at 25 °C with 400 nm excitation wavelength. (Edinburgh Instruments, UK)[3].

Low-Temperature Phosphorescent measurements

Low-temperature phosphorescent measurements were performed using an Edinburgh Instruments FLS1000 spectrometer. Solid powder samples contained in quartz EPR tubes were cooled to 77 K using an Oxford Instruments OptistatDN2 cryostat. Phosphorescence spectra were recorded in time-resolved mode with a xenon lamp and a chopper to gate the long-lived emission. Lifetime decays were acquired via the time-correlated single-photon counting (TCSPC) technique using a microsecond flashlamp (μF900) and fitted after deconvolution with the instrument response function. The absolute phosphorescence quantum yield (Φ_P) at 77 K was determined with an integrating sphere attachment, following a standard procedure based on direct and indirect excitation measurements. The phosphorescence process comprises two steps:

intersystem crossing (ISC) and triplet exciton decay. Its quantum yield(Φ_P) and lifetime(τ_P) are given as follows:

$$\Phi_p = \Phi_{ISC} \times \frac{K_r^p}{K_r^p + K_{nr}^p}$$

$$\tau_p = \frac{1}{K_r^p + K_{nr}^p + K_q^p}$$

Φ_{ISC} is the ISC quantum yield, and K_r^p and K_{nr}^p are the radiative and non-radiative decay rate constants of the T_1 state, K_q^p is environment-induced non-radiative decay rate constant.

Inverted Fluorescence Imaging

Inverted fluorescence microscope (IFM) images were acquired on a Nikon Eclipse Ti-S fluorescent inverted microscope.

Crystallographic Data

The crystal structures of Q[5], Q[6], Q[7], Q[8], TMeQ[6] and HMeQ[6] used for analysis in this work are not new and were obtained from previous studies. The detailed synthesis, crystallization, and single-crystal X-ray diffraction data collection and refinement procedures can be found in the following references: Q[5][1], Q[6][4], Q[7][1], Q[8][1], TMeQ[6][5], HMeQ[6][6]. The corresponding CCDC deposition numbers are [ja993376p for Q[5]], [676880 for Q[6]], [ja993376p for Q[7]], [ja993376p for Q[8]], [2094045 for TMeQ[6]], and [638455 for HMeQ[6]], respectively. These data can be obtained free of charge from The Cambridge Crystallographic Data Centre via www.ccdc.cam.ac.uk/data_request/cif.

Theoretical computational methods

The crystal structure was optimized using the PM7 method implemented in MOPAC2016[7, 8]. To simulate the aqueous solvent environment of cucurbiturils, the COSMO water solvent model was employed for monomers (EPS=78.39, RSOLV=1.3). Single-point energy calculations were performed on the optimized structures using Gaussian 16. The ground state calculations utilized the M06-2X functional of density functional theory with the 6-311G(d,p) basis set. Excited state calculations were

conducted using time-dependent density functional theory with the M06-2X functional and 6-311G(d,p) basis set. The SMD aqueous solvent model was applied to monomers for solvent environment simulation.

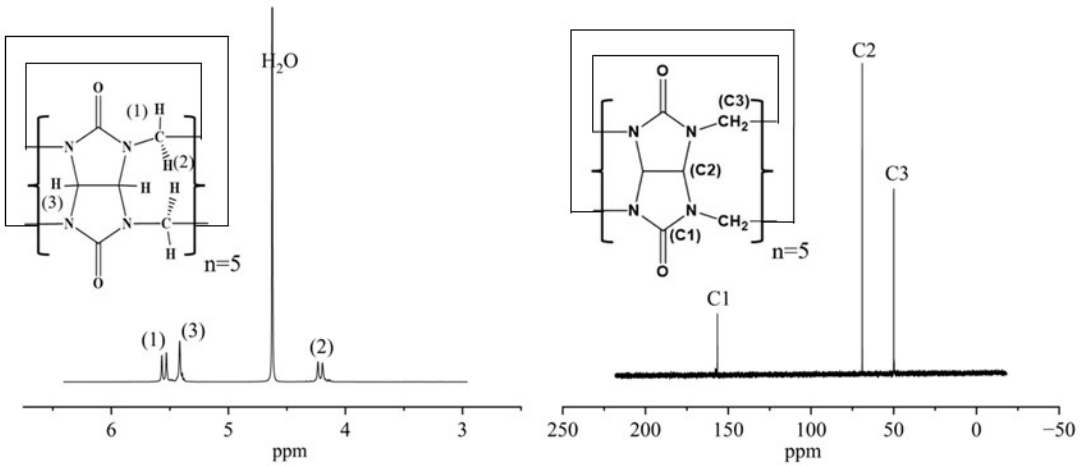

Fig. S1 ^{1}H NMR and ^{13}C NMR spectroscopy of Q[5]

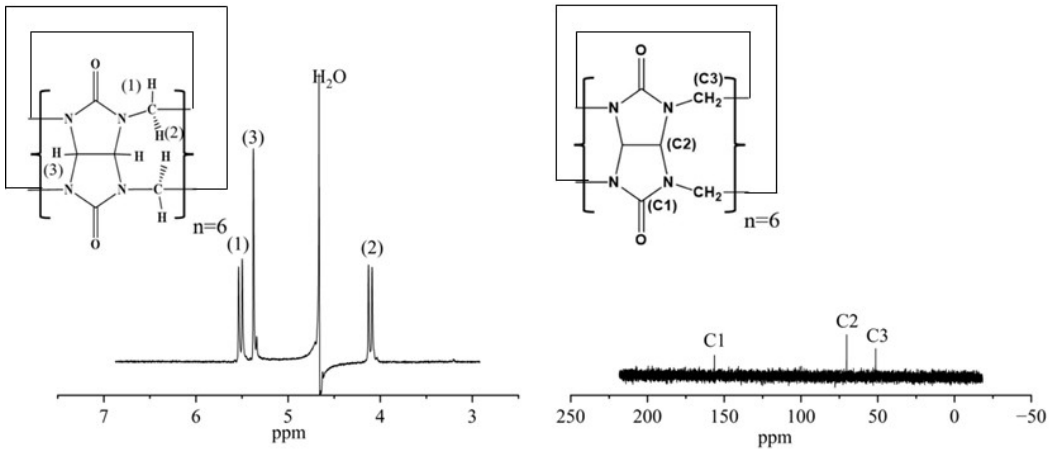

Fig. S2 ^{1}H NMR and ^{13}C NMR spectroscopy of Q[6]

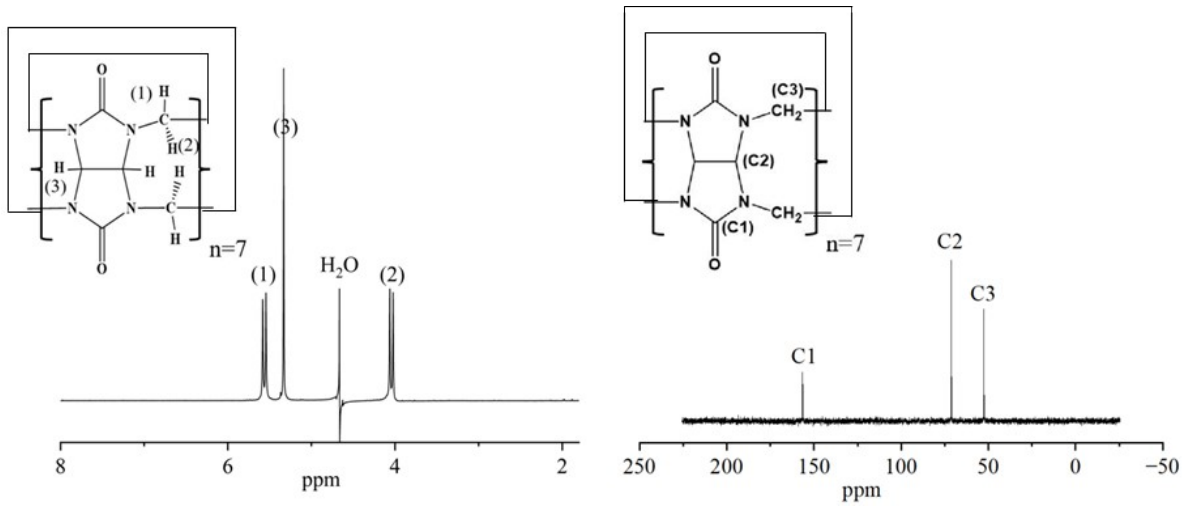

Fig. S3 ^{1}H NMR and ^{13}C NMR spectroscopy of Q[7]

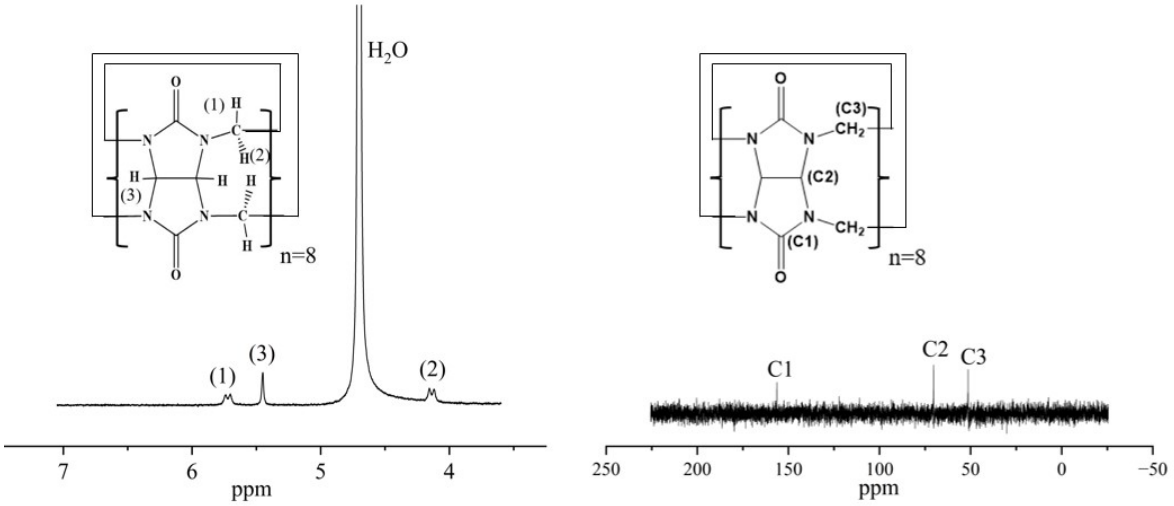

Fig. S4 ^{1}H NMR and ^{13}C NMR spectroscopy of Q[8]

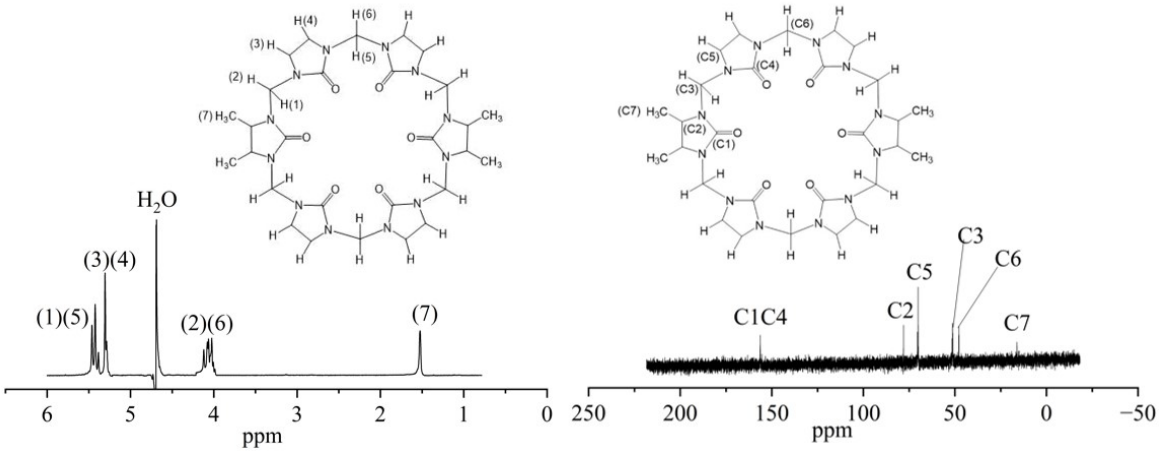

Fig. S5 ^{1}H NMR and ^{13}C NMR spectroscopy of TMeQ[6]

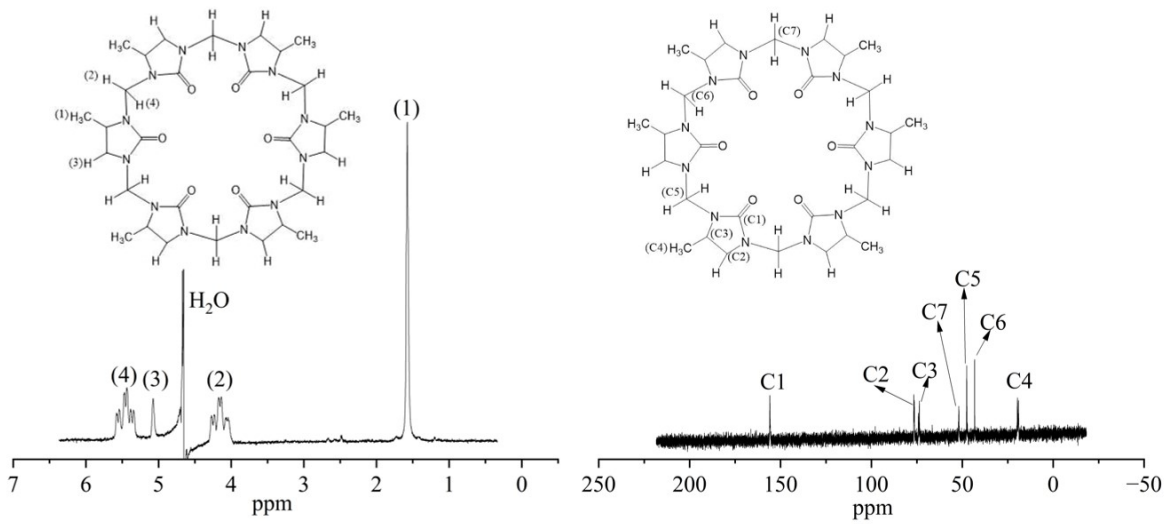

Fig. S6 ^{1}H NMR and ^{13}C NMR spectroscopy of HMeQ[6]

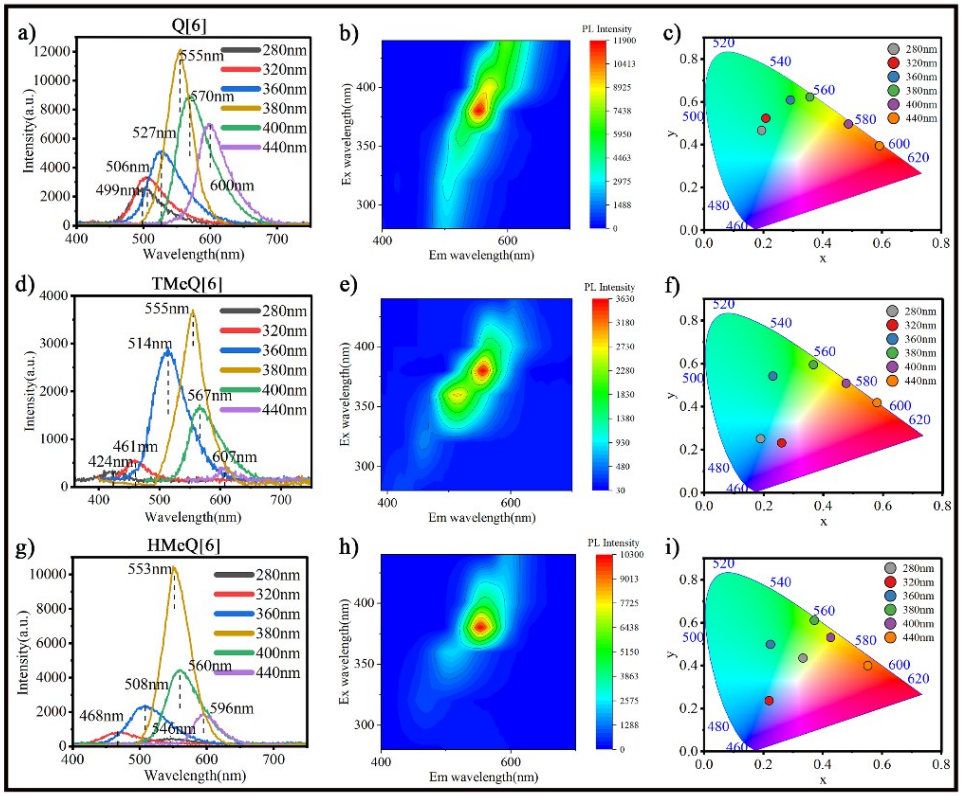

Fig. S7. Low-temperature phosphorescence spectra of Q[6] (a-c), TMeQ[6] (d-f), and HMeQ[6] (g-i) crystals

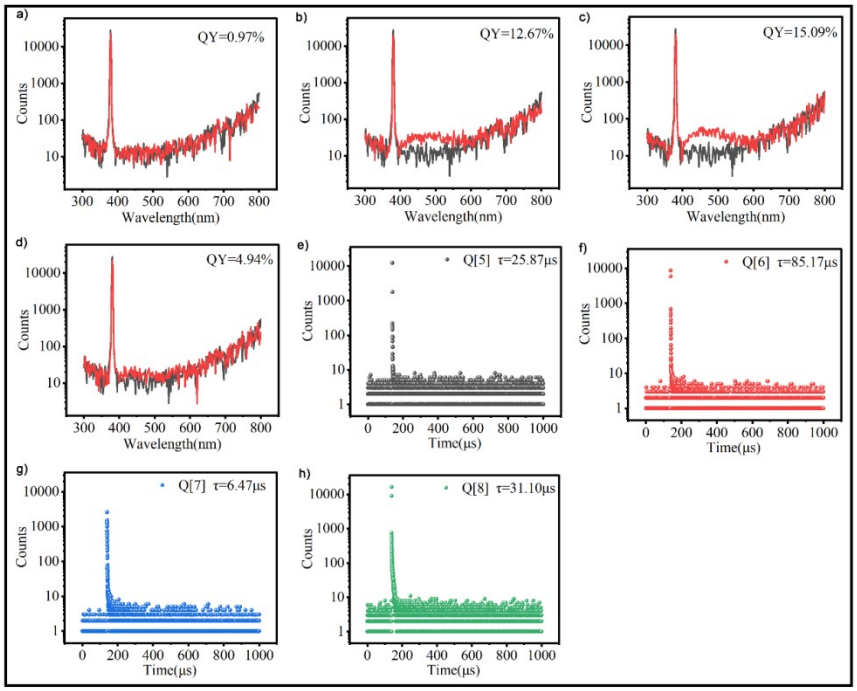

Fig. S8. a-d) Phosphorescence quantum yields and e-h) phosphorescence lifetimes of Q[5]-Q[8] at 77 K (λ_{ex} = 380 nm)

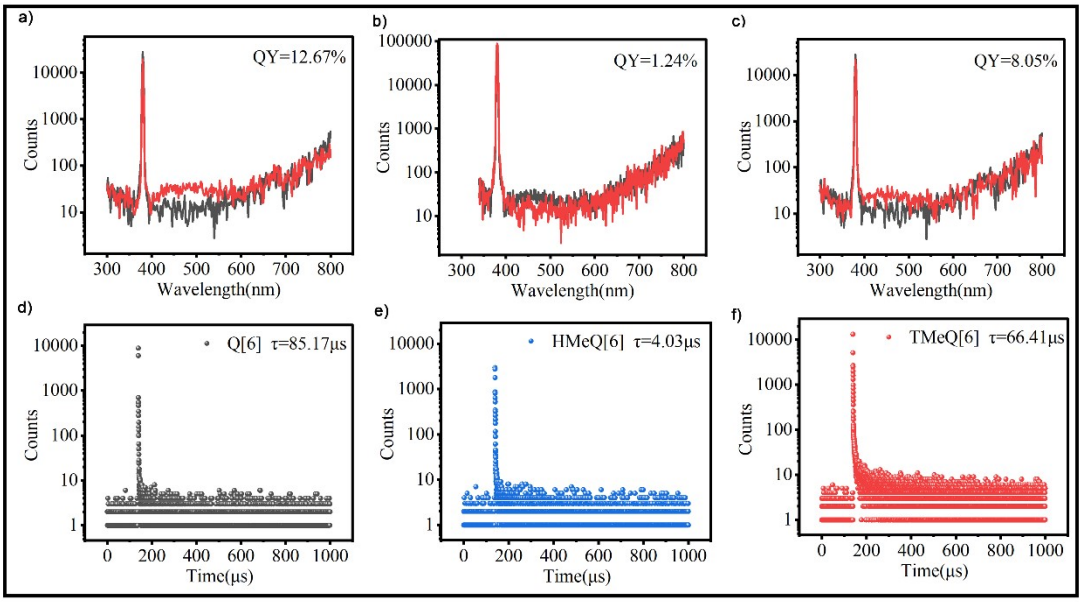

Fig. S9. a-c) Low-temperature phosphorescence quantum yields and e-g) phosphorescence lifetimes of Q[6], HMeQ[6], and TMeQ[6] crystals (λ_{ex}= 380 nm)

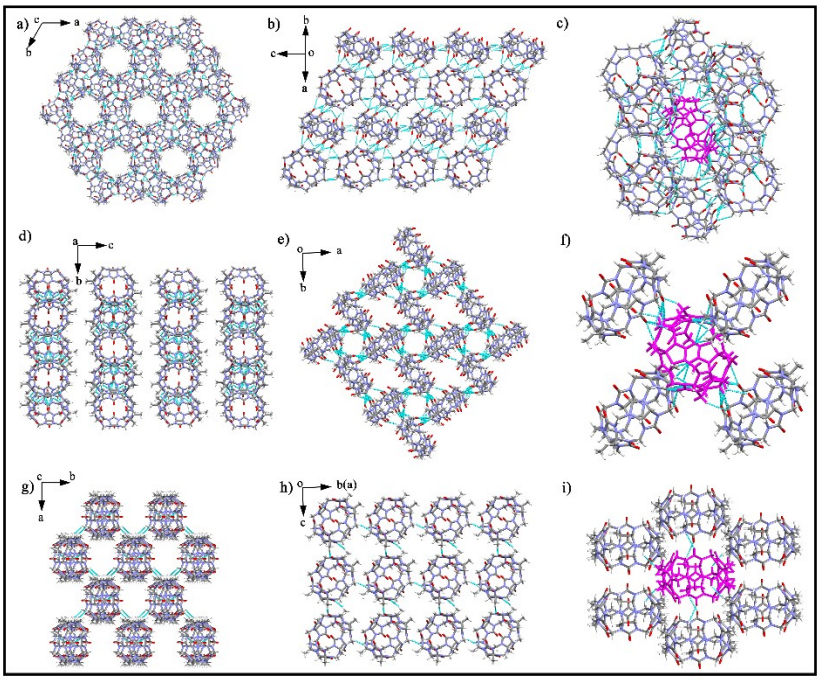

Fig. S10. Crystal structure analysis showing (a-c) three-dimensional architecture, two-dimensional structure, and self-assembly unit count of Q[6]; (d-f) corresponding structural features of TMeQ[6]; (g-i) corresponding structural features of HMeQ[6].

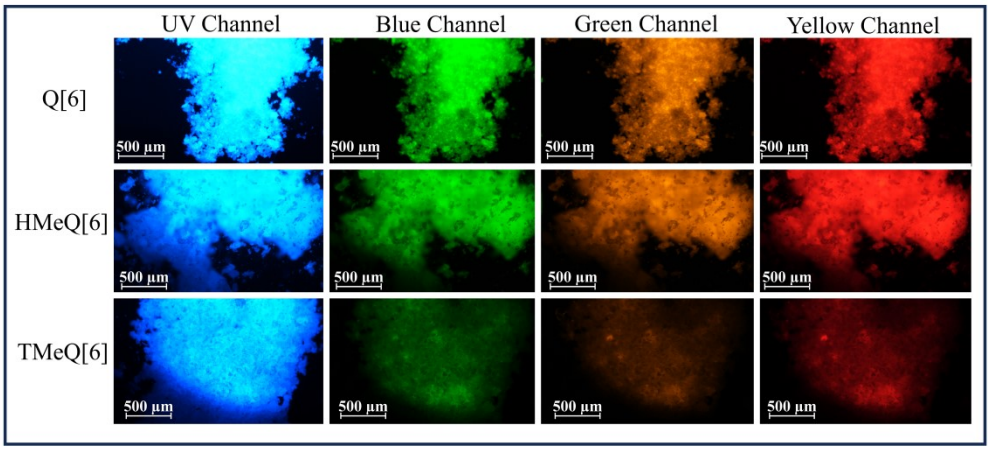

Fig. S11. Photograph of Q[6], HMeQ[6], TMeQ[6] crystals under different channel with Fluorescence inverted microscope

Table S1. Fluorescence quantum yields and lifetimes of Q[5]-Q[8], TMeQ[6], and HMeQ[6] crystals (λ_{ex} = 380 nm)

Powders	Q[5][3]	Q[6][3]	Q[7][3]	Q[8][3]	TMeQ[6][3]	HMeQ[6]

Quantum Yield (%)	4.44%	17.19%	15.33%	10.19%	8.05%	1.24%
Lifetimes(ns)	2.3327	3.0976	5.6512	4.9514	2.8818	0.9021

Table S2. Supramolecular assemblies of Q[5]-Q[8] and their intermolecular interactions

cucurbit[n]uril	Number of self-assembly units	Types and quantities of intermolecular interactions
Q[5]	1+4	-C=O…H_2C (2.666×8，2.699×8，2.243×4 Å)
Q[6]	1+10	1) -C=O…H_2C- (13×2.276，13×2.707，13×2.245，13×2.545，8×2.680 Å) 2) -C=O…CH_2- (13×2.989 Å) 3) -C=O…HC- (13×2.585，13×2.460，13×2.263 Å) 4) -C=O…CH- (13×3.147，13×3.166 Å) 5) - CH_2…H_2C- (12×2.316 Å) 6) -CH_2…CH_2- (12×2.850 Å) 7) -C=O…C=O- (8×3.357 Å)
Q[7]	1+6	1) -C=O…H_2C- (4×2.401，4×2.313，4×2.587，4×2.403 Å) 2) -C=O…CH_2- (4×3.142 Å) 3) -C=O…HC- (4×2.378，4×2.527 Å) 4) -C=O…CH- (4×3.213 Å)
Q[8]	1+4	1) -C=O…H_2C- (4×2.554，4×2.342，4×2.679，4×2.587 Å) 2) -C=O…HC- (4×2.488，4×2.646，4×2.502，4×2.514，4×2.523 Å) 3) -C=O…CH- (4×3.094，4×3.009 Å) 4) -C=O…C=O (4×3.372 Å)

Table S3. Self-assembled aggregates of Q[6], TMeQ[6], and HMeQ[6] and their potential intermolecular interactions

Cucurbit[n]uril	Number of self-assembly units	Types and quantities of intermolecular interactions
Q[6]	1+10	1) -C=O…H_2C- (13×2.276，13×2.707，13×2.245，13×2.545，8×2.680 Å) 2) -C=O…CH_2- (13×2.989 Å) 3) -C=O…HC- (13×2.585，13×2.460，13×2.263 Å) 4) -C=O…CH- (13×3.147，13×3.166 Å) 5) -CH_2…H_2C- (12×2.316 Å) 6) -CH_2…CH_2- (12×2.850 Å) 7) -C=O…C=O- (8×3.357 Å)
TMeQ[6]	1+4	1) -C=O…H_3C- (2.604，2.488，2.604，2.488 Å) 2) -C=O…H_2C- (2×2.653，2×2.522，2×2.568，2×2.670，2×2.673 Å) 3) -C=O…HC- (2×2.356，2×2.530，2×2.606，2×2.343，2×2.377，2×2.717，2×2.532，2×2.350 Å) 5) -C=O…CH- (2×3.008，2×3.049，2×3.196，2×3.118，2×3.032 Å) 6) -C=O…C=O (2×3.241，2×3.259 Å)
HMeQ[6]	1+6	1) -CH_2…H_2C- (4×2.392 Å) 2) -C=O…H_3C- (4×2.569 Å) 3) -C=O…C=O (4×3.429，4×3.467，4×3.438 Å)

Table S4. Electronic energy levels (HOMO, LUMO, S1, T1) of Q[6] monomer and dimer

	HOMO	LUMO	LUMO-HOMO	S_1	T_1	S_1-T_1

Q[6]	-8.17	1.39	9.56	6.7621	6.3025	0.4596
DimerB	-7.95	0.90	8.85	5.9677	5.5558	0.4119

Table S5. Electronic energy levels (HOMO, LUMO, S1, T1) of Q[7] monomer and dimer

	HOMO	LUMO	LUMO-HOMO	S_1	T_1	S_1-T_1
Q[7]	-8.17	1.39	9.56	6.7663	6.2799	0.4864
DimerB	-7.16	0.71	7.87	6.0295	5.6193	0.4102

Table S6. Electronic energy levels (HOMO, LUMO, S1, T1) of HMeQ[6] monomer and dimer

	HOMO	LUMO	LUMO-HOMO	S1	T1	S1-T1
HMeQ[6]	-8.12	1.47	9.59	6.7753	6.2096	0.5657
DimerB	-7.3	0.98	8.28	6.1958	5.7648	0.431

Reference

1. J. Kim, I.-S. Jung, S.-Y. Kim, E. Lee, J.-K. Kang, S. Sakamoto, K. Yamaguchi and K. Kim, *J. Am. Chem. Soc.*, 2000, **122**, 540-541.
2. Y. Zhao, S. Xue, Q. Zhu, Z. Tao, J. Zhang, Z. Wei, L. Long, M. Hu, H. Xiao and A. Day, *Chin. Sci. Bull.*, 2004, **49**, 1111-1116.
3. K.-N. Wei, Q.-J. Zhang, Y.-Q. Zhang, X. Zeng, X. Xiao, Y. Huang, K. Chen and Z. Tao, *Spectrochim. Acta, Part A*, 2022, **272**, 121015.
4. S. Lim, H. Kim, N. Selvapalam, K.-J. Kim, S. J. Cho, G. Seo and K. Kim, *Angew. Chem.*, 2008, **120**, 3400-3403.
5. R.-X. Cheng, F.-Y. Tian, L.-X. Chen, Q.-J. Zhu, K. Chen and Z. Tao, *Cryst. Growth Des.*, 2022, **22**, 747-750.
6. J. Lin, Y. Zhang, J. Zhang, S. Xue, Q. Zhu and Z. Tao, *J. Mol. Struct.*, 2008, **875**, 442-446.
7. M.J. Frisch, G.W.Trucks, H.B.Schlegel, G.E.Scuseria, M.A. Robb, J.R.Cheeseman,

G.Scalmani, V.Barone, G.A.Petersson, H.Nakatsuji, X.Li, M.Caricato, A.V.Marenich, J.Bloino, B.G.Janesko, R. Gomperts, B. Mennucci, H.P.Hratchian, J.V.Ortiz, A.F.Izmaylov, J.L.Sonnenberg, D.Williams-Young, F.Ding, F.Lipparini, F.Egidi, J.Goings, B.Peng, A. Petrone, T.Henderson, D.Ranasinghe,V. G. Zakrzewski, J.Gao, N.Rega, G.Zheng, W.Liang, M.Hada, M.Ehara, K.Toyota, R.Fukuda, J.Hasegawa, M.Ishida, T.Nakajima, Y.Honda, O.Kitao, H.Nakai, T.Vreven, K.Throssell, J.A.Montgomery, Jr.J.E. Peralta, F.Ogliaro, M.J.Bearpark, J.Heyd, E.N.Brothers, K.N.Kudin, V. N. Staroverov, T. A. Keith, R. Kobayashi, J.Normand, K.Raghavachari, A.P.Rendell, J.C.Burant, S.S.Iyengar, J.Tomasi, M.Cossi, J.M.Millam, M.Klene, C.Adamo, R. Cammi,J.W. Ochterski, R.L.Martin,K.Morokuma, O.Farkas, J.B.Foresman, and D. J. Fox, Gaussian 16, Revision A. 03; Gaussian, Inc, Wallingford CT, 2016.

8. J.J.P. Stewart, MOPAC 2016 (Molecular Orbital PACkage). http://openmopac.net/MOPAC2016.html (accessed July 29, 2017).